Hysteresis Between Canopy Temperature and Atmospheric Temperature and Their Drivers on Winter Wheat

Jialiang Huang
Shuang Wang
Yuhong Guo
Junying Chen (junyingchen@nwafu.edu.cn)
Northwest A&F University: Northwest Agriculture and Forestry University
Yifei Yao
Dianyu Chen
Qi Liu
Yuxin Zhang
Zhitao Zhang
Youzhen Xiang

Research Article

Keywords: time-lag effect, canopy temperature, atmospheric temperature, soil moisture, meteorological factors

Posted Date: March 11th, 2022

DOI: https://doi.org/10.21203/rs.3.rs-1423258/v1

Hysteresis Between Canopy Temperature and Atmospheric Temperature and Their Drivers on Winter Wheat

Jialiang Huang [a,b] Shuang Wang [a,b] Yuhong Guo [a,b] Junying Chen [a,b,*] Yifei Yao [a,b,*] Dianyu Chen [a,b] Qi Liu [a,b] Yuxin Zhang [a,b] Zhitao Zhang [a,b] Youzhen Xiang [a,b]

[a] Key Laboratory of Agricultural Soil and Water Engineering in Arid and Semiarid Areas of Ministry of Education, Northwest A&F University, Yangling 712100, China

[b] Institute of Water-Saving Agriculture in Arid Areas of China, Northwest A&F University, Yangling 712100, China

[*] Corresponding to: College of Water Resources and Architectural Engineering, Northwest A&F University, Yangling 712100, Shaanxi, China.

E-mail addresses: junyingchen@nwafu.edu.cn (Junying Chen), yifeiyao@nwsuaf.edu.cn (Yifei Yao)

Abstract: Quantitative characterization of the time-lag effect between canopy temperature and atmospheric temperature and its controlling factors in the agricultural ecosystem may contribute to a higher inversion accuracy of soil water content using canopy-air temperature information. For this end, the canopy temperature (Tc) of winter wheat at four irrigation levels, W1 (field capacity of 95%), W2 (field capacity of 80%), W3 (field capacity of 65%) and W4 (field capacity of 50%), were continuously monitored, and the data of such environmental factors as solar radiation (Rs), atmospheric temperature (Ta), relative humidity (RH) and soil water content (SWC) were simultaneously collected. With the synchronous diurnal time series, the lag relationship between Tc and Ta was analyzed, and the lag time (LT) was calculated using time-lagged correlation analysis; multiple linear regression model was used to construct the time lag model based on factors of Rs, Ta, RH and SWC, and path analysis was used to study the interaction among the factors. The results showed: (1) hysteresis existed between Tc and Ta over the diel cycles, and different weather and irrigation levels did not change the direction of the time lag loop. (2) the key driver regulating the diel hysteresis pattern between Tc and Ta varied under different weather: on rainy days, key driver was Rs while on cloudy and sunny days, the key driver was RH. Meanwhile, SWC had some effect on hysteresis under a certain threshold.(3) the multiple regression model indicated that together Rs, Ta, RH, and SWC explained 68±3, 48±8, and 64±3% of the variation of time-lag effect on rainy, cloudy, and sunny days, respectively. Path analysis showed that the key driver could enhance the time-lag effect through other indirect factors. These findings clearly indicated a dynamic process of time-lag effect between Tc and Ta with different weather and different irrigation levels. This study contributes to the understanding of the time-lag effect and its driving factors and this analysis provides the basis for further improvement on monitoring crop water deficit.

Key word: time-lag effect; canopy temperature; atmospheric temperature; soil moisture; meteorological factors

1 Introduction

The limited water resources and their low utilization ratio are two important factors restricting the development of agriculture in China (Zhai et al., 2003). Timely and accurate monitoring or diagnosis of crop water status is vital to improve agricultural water management, water use efficiency and water-saving precision irrigation agriculture (Gerhards et al., 2018). The inversion

of crop moisture is mainly based on Tc or Tc- Ta difference (Clawson et al., 1989; Jackson et al., 1981), but the response of Tc to Ta has a certain time-lag effect, resulting in low diagnosis accuracy of crop water information and limited application (Biju et al., 2018). Therefore, to study the influence mechanism of time-lag effect can effectively improve crop water diagnosis accuracy.

As an important parameter in water and heat exchange between soil, crop and atmosphere (Jackson et al., 1981), Tc represents the average surface temperature of crop canopy and reflects the energy exchange between crops and their atmosphere (Clawson et al., 1989),. During heat exchange, Rs absorbed by the canopy is decomposed into latent heat flux and sensible heat flux (Tamai et al., 1998). It is sensible heat flux rather than Latent heat flux that change the canopy surface temperature (Baker et al., 2001). Relevant studies have found a difference in the absorption of solar shortwave radiation by vegetation and air (Alados et al., 2003). The absortion of net solar radiation warms up the canopy, which releases energy to increase the surrounding temperature via long-wave radiation. In consequence, the peaks of Tc and Ta are not synchronized (Lu et al., 2008). This phenomenon is a certain hysteresis (Zhang et al., 2018b). LT is a hysteresis that is defined as the time difference between peak values between plant physiology index and meteorological variables (Wang et al., 2019), and the length and direction of a time lag can, in turn, reflect the magnitude of hysteresis (Zhang et al., 2014).

Recently, increasing studies have found that the responses of vegetation to climate have a hysteresis (Davis, 1989; Kuzyakov and Gavrichkova, 2010; Saatchi et al., 2013; Vicente-Serrano et al., 2013). Chen et al. (2014) have indicated that the diel hysteresis pattern between Tc and Ta is attributed to strong correlation between temperature and environmental factors. For example, soil moisture has some effect on Tc, and Tc increases rapidly under water stress (Jackson et al., 1981), and soil moisture influences the diel hysteresis pattern between Tc and Ta (Tuzet et al., 2003). Besides, as Tc depends on sensible and latent heat equilibrium in plants (Baker et al., 2001), solar radiation is a key environmental driver of the diel hysteresis pattern (Wu et al., 2015; Zhang et al., 2019). Meanwhile, higher humidity has a cooling effect on crops, which will possibly result in the change of the diel hysteresis pattern (Anderson et al., 2010; Wang et al., 2019). Although a wealth of studies are available about the time-lag effect of plant physiological indexes and environmental factors, most of them focus on the description of hysteresis phenomenon or the analysis of the correlation between single factor and time-lag effect (Bo et al., 2017; Jiang et al., 2022; Zhang et al., 2014), and lack the analysis of how environmental factors influence time-lag effect under different weather.

In this study, experiment was conducted on winter wheat in the arid and semi-arid region of northwest of China from October 2020 through June 2021. By investigating the temporal dynamic of Tc and Ta with different weather and irrigation levels, the objectives of the present study were to (i) quantify the time-lag effect between Tc and Ta through LT, (ii) analyze the quantitative effects of environmental factors on time-lag effect.

2 Materials and Methods

2.1 Study Site Description

The study area is located at the Key Laboratory of Agricultural Soil and Water Engineering in Arid and Semiarid Areas of Ministry of Education of China (108°4'20"E, 34°17'42.17"N). The average annual rainfall in this area is 635 mm, and the rainfall is mainly concentrated from July through September. The soil (0–60 cm) is medium loam, with an average field capacity (FC) of 26% and a wilting coefficient of 8.6%. The dry bulk density, pH value, organic matter content, and total

nitrogen content of the soil are 1.44 g/cm^3, 8.1, 13.3 g/kg, and 0.82 g/kg, respectively. The mean annual meteorological data for the trial site and the soil properties within the 0–60 cm of soil are described in Table 1.

Table 1 Mean annual meteorological data at the experimental site and the properties of the topsoil (0–60 cm) in the experimental field.

Item	Content	Annotation
mean annual precipitation (mm)	635	2010–2018（About 60% is concentrated from July to September）
Mean annual air temperature (◦C)	12.9	Air temperature is usually lowest in January
mean annual pan evaporation (mm)	1500	
mean annual sunshine hours (h)	2164	
mean annual frost-free period (d)	210	
Soil dry bulk density (g cm^{-3})	1.44	The core sampling method by using a ring knife
Field capacity (%)	26.0	Gravity moisture content; Ring knife method
Permanent wilting point (%)	8.6	Gravity moisture content; Ring knife method
Soil organic matter(g kg^{-1})	13.3	Determined by dichromate wet oxidation
Total nitrogen (g kg^{-1})	0.82	Determined by Kjeldahl distillation titration
PH	8.1	Acid - Alkali indicator method

2.2 Experiment Design

The layout of the experimental plots was completely random, and the planting time was October 18, 2020. As is shown in Fig.1, four irrigation levels were set, and the irrigation limits were set as W1 (the control group, field capacity of 95%), W2 (field capacity of 80%), W3 (field capacity of 65%) and W4 (field capacity of 50%). Each irrigation level had three repeats, and altogether there were 12 plots. The four different treatments were: full irrigation (W1), mild water stress (W2), moderate water stress (W3) and severe water stress (W4). Nitrogen fertilizer and phosphate fertilizer (240 kg/ha, respectively) were applied as base fertilizer before sowing. The winter wheat was a variety named Xiaoyan 22 popularized in central Shaanxi Province. The plots (4 m × 4 m) had a row spacing of 0.25 m and a density of 1 million plants/ha. Winter wheat was irrigated using a drip system with one line per row, and the drippers, which had a flow rate of 1.2 L/h, were spaced at intervals of 0.1 m.

Fig 1.Overview of the experimental site

Drip irrigation was used in each experimental plot, and a drip irrigation belt was laid on each row of crops to ensure the uniformity of irrigation. Before each irrigation, soil samples of 5 depths (10, 20, 30, 40 and 60 cm) were collected by soil drilling drill and dried for 8 hours at 105℃ (Zhou et al., 2021). The mass water content of soil corresponding to each depth was calculated according to

the difference in the change of drying weight. Based on SWC measured by drying method, the irrigation amount is strictly controlled through water meter for each plot until the corresponding irrigation upper limit is reached. The irrigation amount and irrigation dates are shown in Table 2, and the whole growth period of winter wheat was irrigated 3 times. The calculation formula (Ru et al., 2020) for irrigation quota (M) is expressed as follows:

$$M = 1000\gamma_s HP(\beta_1 - \beta_2) \quad (1)$$

Where M is the irrigation quota (mm); $\gamma_s$is the apparent density, which is numerically equal to the soil bulk density, dimensionless, 1.44; H is the depth of the wet layer (m), 0.4 m; P is the wetness ratio of the drip irrigation, dimensionless, 0.8; β_1 is the upper limit of the soil moisture content (mass) (%), which is the soil field capacity, 26.0; and β_2 is the lower limit of the soil moisture content (mass) (%).

Table 2 Irrigation amount of winter wheat at different growth stages.

Growth stage	Irrigation date	Irrigation quota(mm)			
		W1	W2	W3	W4
Wintering stage	19/12/2020	23	16	10	0
Returning green stage	5/3/2021	37	32	29	0
Jointing stage	15/5/2021	25	15	7	0
Total irrigation amount		95	63	46	0

2.3 Data Acquisition

2.3.1Tc measurements

Continuous Tc monitoring data a sophisticated infrared thermometer SI-411 produced by Apogee Company was used to continuously monitor Tcchanges during wheat growth period at an interval of 2 minutes. The SI-411 infrared thermometer was set to record observations directly above the canopy of four plots W1, W2, W3 and W4, and the distance between it and the canopy was set at 1 meter. The sensor has SDI-12 digital output. With a field of view of 22° and a response time of 0.1 seconds, the temperature condition of the monitoring point can be continuously measured. Tc changes of wheat during the whole growth period were obtained by continuous monitoring.

2.3.2 Environmental factors measurements

The measurements of environmental factors were conducted by an automatic weather station located in the winter wheat pilot area. Meteorological sensors were installed to observe environmental factors (Table 3), including solar radiation (Rs), atmospheric temperature (Ta), relative humidity (RH), wind speed (u), soil heat flux (G), soil water content (SWC) and precipitation (P). All the sensors were calibrated at the beginning of 2020 and recorded at 2-min intervals.

Table.3 Summary of environmental factors observed by the weather station

Variables	Sensor number	Instrument height(m)	Abbreviation	Unit
Solar radiation	SN-500	3.5	Rs	W m^{-2}
Soil heat flux	HFP01	-0.10	G	W m^{-2}
Air temperature	HC2AS3	2.5	Ta	℃
Relative humidity	HC2AS3	2.5	RH	%
Soil water content	TDR-315H	-0.10, -0.20, -0.40	SWC	%
Wind speed		2	u	m s^{-1}
Precipitation			P	mm

Note: SWC was measured at three positions. Measurements were conducted using sensors at depths of 0.10, 0.20 and 0.40 m, respectively. An average of the three SWC measurements represents the mean SWC.

2.4 Data Processing

2.4.1 Dislocation Movement Method

The Time-lagged Correlation between Tc and Ta was analyzed by the dislocation movement method (Zhang et al., 2019; Zhao et al., 2006). Specifically, the diurnal variation of Tc was similar to that of Ta. The synchronous time series of Tc and Ta data moves with a time step of 2 minutes, and the correlation coefficient of the two series was calculated. It was considered that the corresponding translation time was LT when the correlation coefficient was the maximum. Calculation formula of correlation coefficient:

$$R_{\mathrm{m}}=\frac{\sum_{\mathrm{i=1}}^{\mathrm{n-m}}(x_i-\bar{x})(y_i-\bar{y})}{\sqrt{\sum_{i=1}^{n-m}(x_i-\bar{x})^2}\sqrt{\sum_{i=1}^{n-m}(y_i-\bar{y})^2}} \quad (2)$$

Where R was the correlation coefficient, x and y respectively represented Tc and Ta, n was the number of samples, and m was the number of dislocation.

The lag correlation coefficient was calculated as follows:

$$R_{\mathrm{n}}=\max(R_{-m},\Lambda\ R_{-2},R_{-1},R_0,R_1,R_2,\Lambda\ R_{\mathrm{m}}) \quad (3)$$

Where the maximum value is the lag correlation coefficient, represented by R_n, then LT between Tc and Ta was 2* N minutes. In this study, LT between Tc and Ta factor positive or clockwise circulation meant Tc peak earlier than Ta; LT between Tc and Ta negative or counterclockwise circle meant Tc peak later than Ta.

2.4.2 Linear regression analysis

Linear regression is a statistical analysis method that uses regression analysis in mathematical statistics to determine the interdependent quantitative relationship between two or more variables, which is widely used (Seber and Lee, 2012; Tranmer and Elliot, 2008). In this study, the effect of environmental factors (Rs, Ta, RH and SWC) on time-lag effect was analyzed by linear regression. In order to study the dynamic changes of time lag in different weather, the regression slope is used to represent the sensitivity of time-lag effect to changes in environmental factor parameters(Hayat et al., 2020).

2.4.3 Path analysis theory

Path analysis is one of the typical multivariate statistical analysis methods to study relationships among numerous variables (Khazaie et al., 2011; Zhang et al., 2016). This method can elucidate the degree of the direct effect of independent variables on the dependent variables, as well as the indirect effect of one independent variable on the dependent variables through other independent variables (Khazaie et al., 2011; Sun et al., 2020). A detailed description can be found in the references (Khazaie et al., 2011; Xing et al., 2016). In this study, the path analysis method was applied to determine the relative direct and indirect effects of environmental factors on time-lag effect between Tc and Ta.

3 Results

3.1 Dynamics of Tc and environmental factors

The main growth period of winter wheat was from December through June, which mainly includes jointing, heading and filling stages. The dynamic curve of daily mean value of Tc and environmental factors were shown in Fig.2. Rs fluctuated less in winter, basically between 0 and 100W/m^2, while in spring and summer, Rs fluctuates more, up to 200 W/m^2. With the seasonal change, Ta showed an upward trend, from -5 to 30 ℃. There was basically no precipitation from December to January, so RH was maintained at 30~60%. Most of the precipitation was concentrated in February to May, and RH was relatively high, maintaining above 40%. The Tc of four different irrigation levels also showed a rising trend with seasonal change. SWC decreased with time, but increased sharply after irrigation.

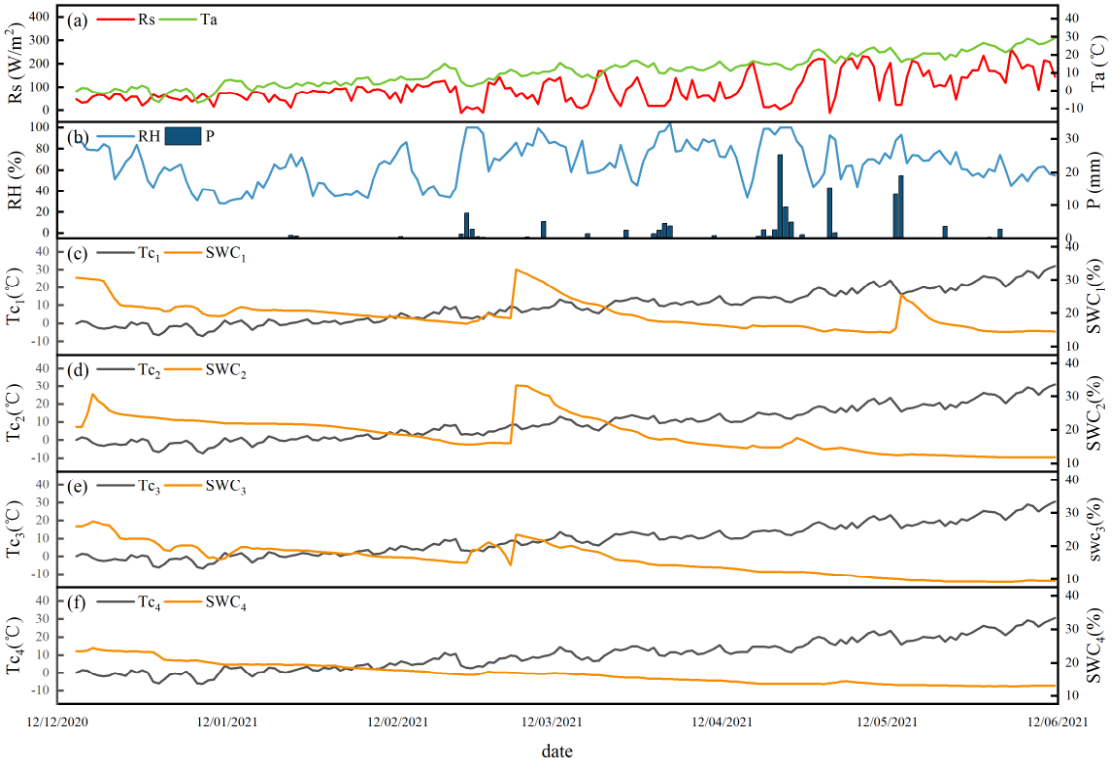

Fig.2. Dynamic variation of (a) daily average Rs and Ta; (b) daily average RH and P (P is the total daily rainfall); (c) daily average Tc_1 and SWC_1; (d) daily average Tc_2 and SWC_2; (e) daily average Tc_3 and SWC_3; (f) daily average Tc_4 and SWC_4.

The response pattern characteristics of Tc and Ta among rainy (April 4, 2021), cloudy (April 18, 2021) and sunny day (April 15, 2021) were analyzed, and the results were shown in Fig 3. As shown in the figure, the diurnal variation of Tc and Ta of winter wheat showed a clockwise trend. There was little difference in the time when the Tc began to rise under different weather; most of them began to rise between 5:00 and 6:00, but the peak time of Tc under different weather showed significant differences. The Tc reached its peak at 14:51 ± 17, 14:02 ± 18, and 12:28 ± 10 among rainy, cloudy, and sunny days, respectively. As the weather improved better, Tc peaked somewhat earlier. This possibly was because with better weather and higher net effective radiation hitting vegetation, it was easier for vegetation to achieve latent and sensible heat energy balance, and therefore Tc peaked earlier. Under different weather, Ta started rising around 5:30, but peaked at 15:38, 14:58, and 13:18 on cloudy, rainy, and sunny days, respectively. Meanwhile, Ta also showed a trend of rising first and then decreasing, but the peak time of Ta was much later than the

peak time of Tc, and there were peak time differences (49 ± 17, 56 ± 18, and 50 ± 10 min). Therefore, on the whole, the peak Ta lagged behind the peak Tc.

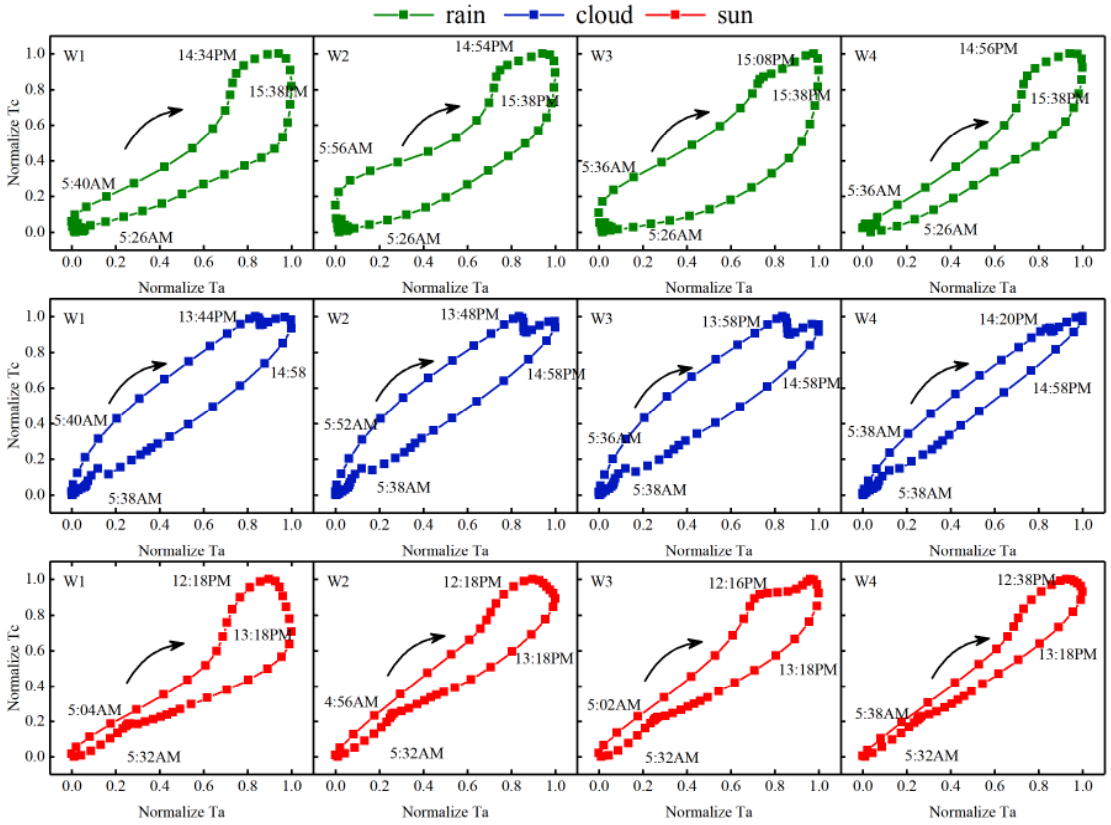

Fig. 3. The loop of Tc and Ta on rainy day(April 4, 2021),cloudy day (April 18, 2021) and sunny day (April 15, 2021).

3.2 LT between Tc and Ta under different weather

LT of Tc and Ta was calculated according to formulas (2) and (3), and classified statistics were made according to different weather (Fig.4). On cloudy days, LT of W1, W2, W3 and W4 narrowed to a certain extent with the decrease of irrigation level. The lower limit of LT of the four irrigation levels had little difference, basically ranging from 0 to 12min. But the upper limit of LT of the four irrigation levels had significant differences, while, the upper limit of LT of W4 decreased by nearly 20 min than that of W1, W2 and W3. Similar to the result of rainy days, LT showed a narrowing trend with the decrease of irrigation level under cloudy weather. Besides, LT of W1, W2 and W3 varied from 30 to 80 min, while LT of W4 varied from 14 to 64 min. LT fluctuation range of W4 was significantly higher than that of the cloudy day, which was nearly increased by 10 to 20 min. On sunny days, the time lag kept narrowing with the decrease of irrigation level. LT upper limit of W1, W2 and W3 was around 80 min, while LT upper limit of W4 was around 66min. LT lower limit of sunny days was between cloudy days and cloudy days.

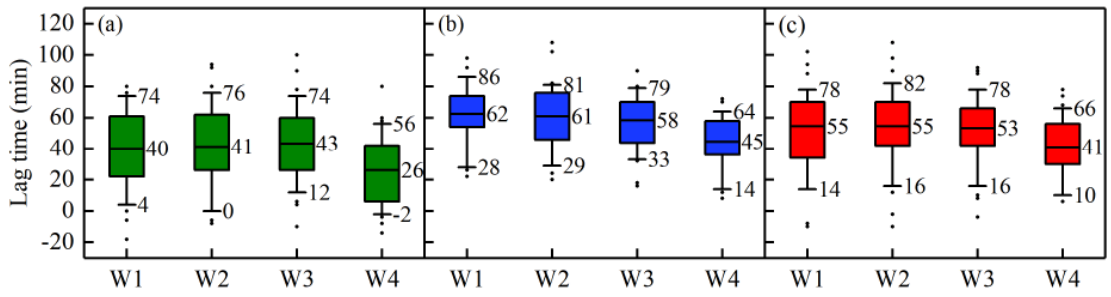

Fig. 4. LT between Tc and Ta under different weather.

3.3 Relationships between TL and environmental factors

Scatter plot (Fig.5) was used to describe LT between Tc and Ta on cloudy days and the correlation between daily environmental factors. LT and environmental factors under different water treatments showed a similar trend, except SWC. There was no significant correlation between LT and SWC under W1, W2 and W3 irrigation levels (R^2 <0.10, P>0.05), while there was a positive correlation between LT and SWC under W4 irrigation level (R^2=0.260, P<0.05). LT was positively correlated with daily mean Rs, and the determination coefficient R^2 was generally above 0.50, reaching significant level (P<0.01). In addition, LT and daily mean Ta and RH were negatively correlated, while determination coefficient R^2 was above 0.21 and 0.16, respectively, reaching significant level (P<0.01). Under cloudy weather, LT was mainly controlled by Rs, and was affected by Ta and RH. Only at lower irrigation level did it have some effect on LT.

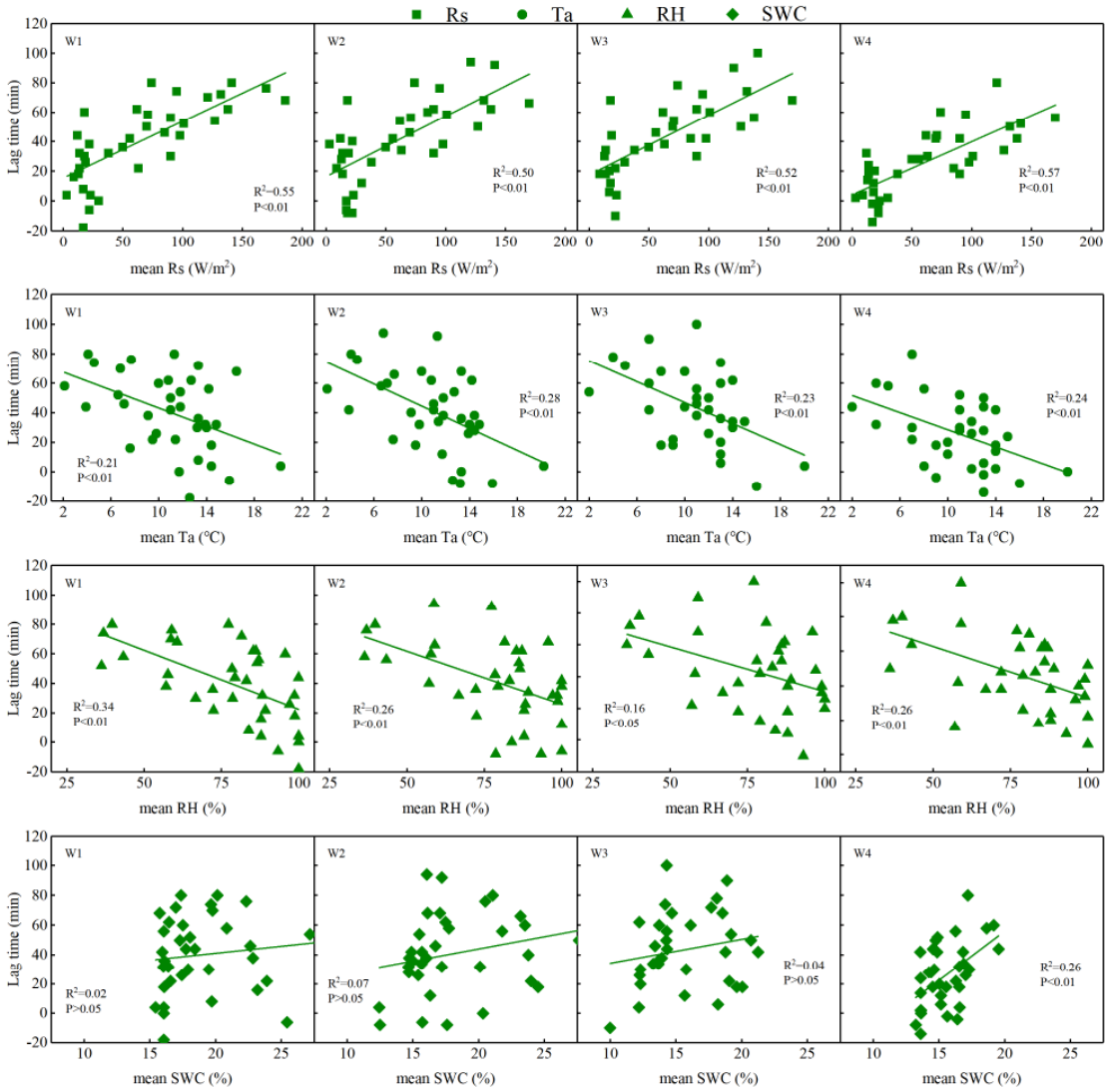

Fig.5. Relationship between LT and environmental factors on rainy days

The relationship between LT and environmental factors on cloudy days was different from that on rainy days (Fig.6). There was no significant correlation between LT and daily Rs (R^2<0.02). In addition, the correlation of LT and daily Ta under W1, W2 and W3 irrigation levels (R^2= 0.07, 0.01 and 0.14) was not as high as that W4 irrigation level (R^2=0.29). LT and daily RH was

positively correlated, which determination coefficient R^2 was above 0.29, reaching a significant level ($P<0.01$). On the other hand, the lag time and SWC was similar to that on rainy days, but the lag time and SWC was further correlated under W4 irrigation level, the determination coefficient R^2 was 0.36. It indicated that LT was controlled by RH under cloudy weather, but was not affected by Rs.

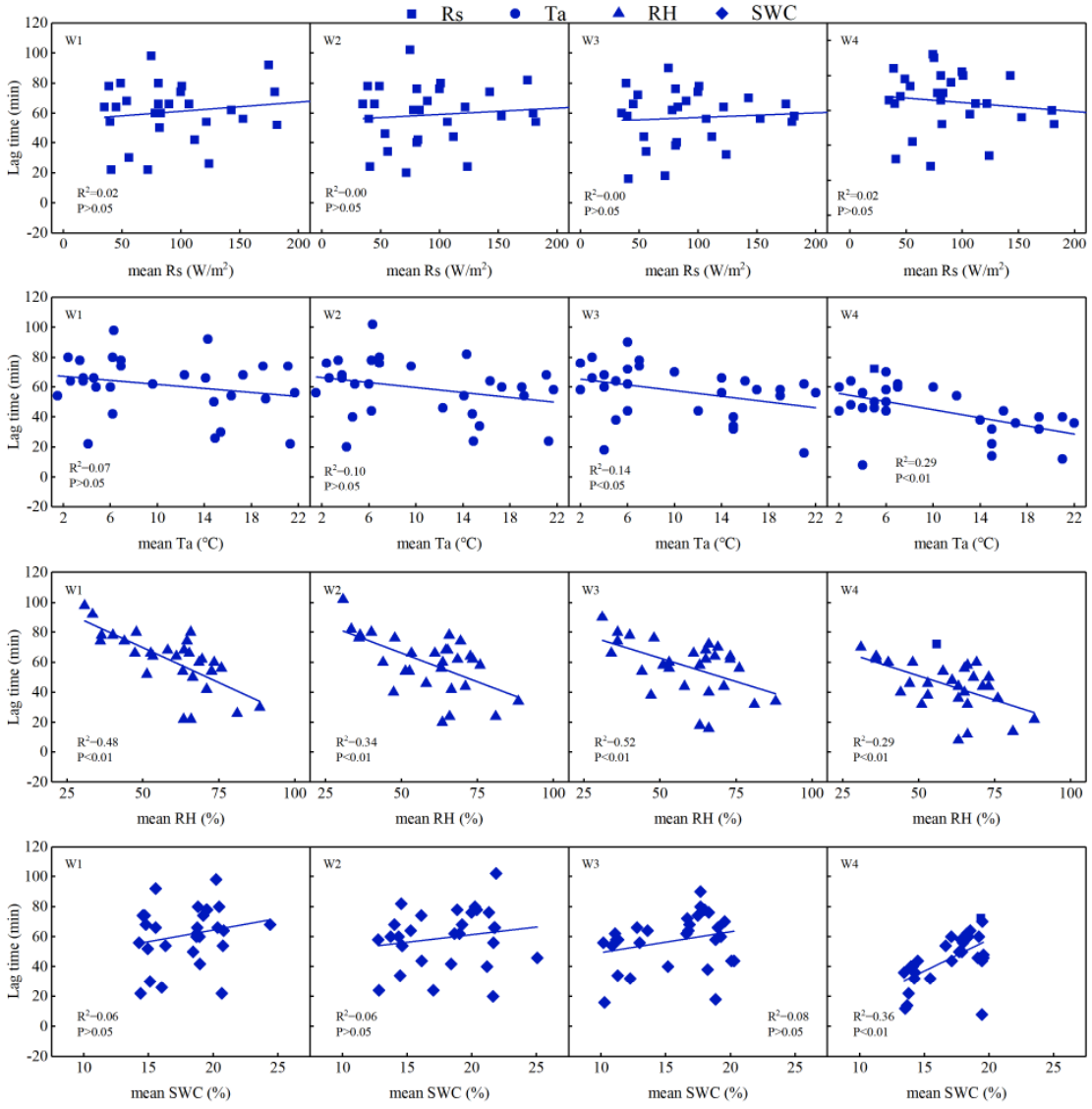

Fig.6. Relationship between LT and environmental factors on cloud days

The relationship between LT and environmental factors on sunny days was similar to that on cloudy days. There was no significant correlation between LT and daily Rs ($R^2<0.05$). The correlation between LT and daily Ta under W1, W2 and W3 irrigation level (R^2= 0.00, 0.10 and 0.12) was not as high as that of W4 irrigation level (R^2=0.27). The correlation between LT and daily RH was significantly positive, while the correlation was much higher than that of cloudy days, when the determination coefficient R^2 was above 0.48 ($P<0.01$). It indicated that LT was further controlled by RH on sunny days. If water treatment is low, it also was affected by Ta and SWC under low irrigation level, which was not obviously affected by Rs.

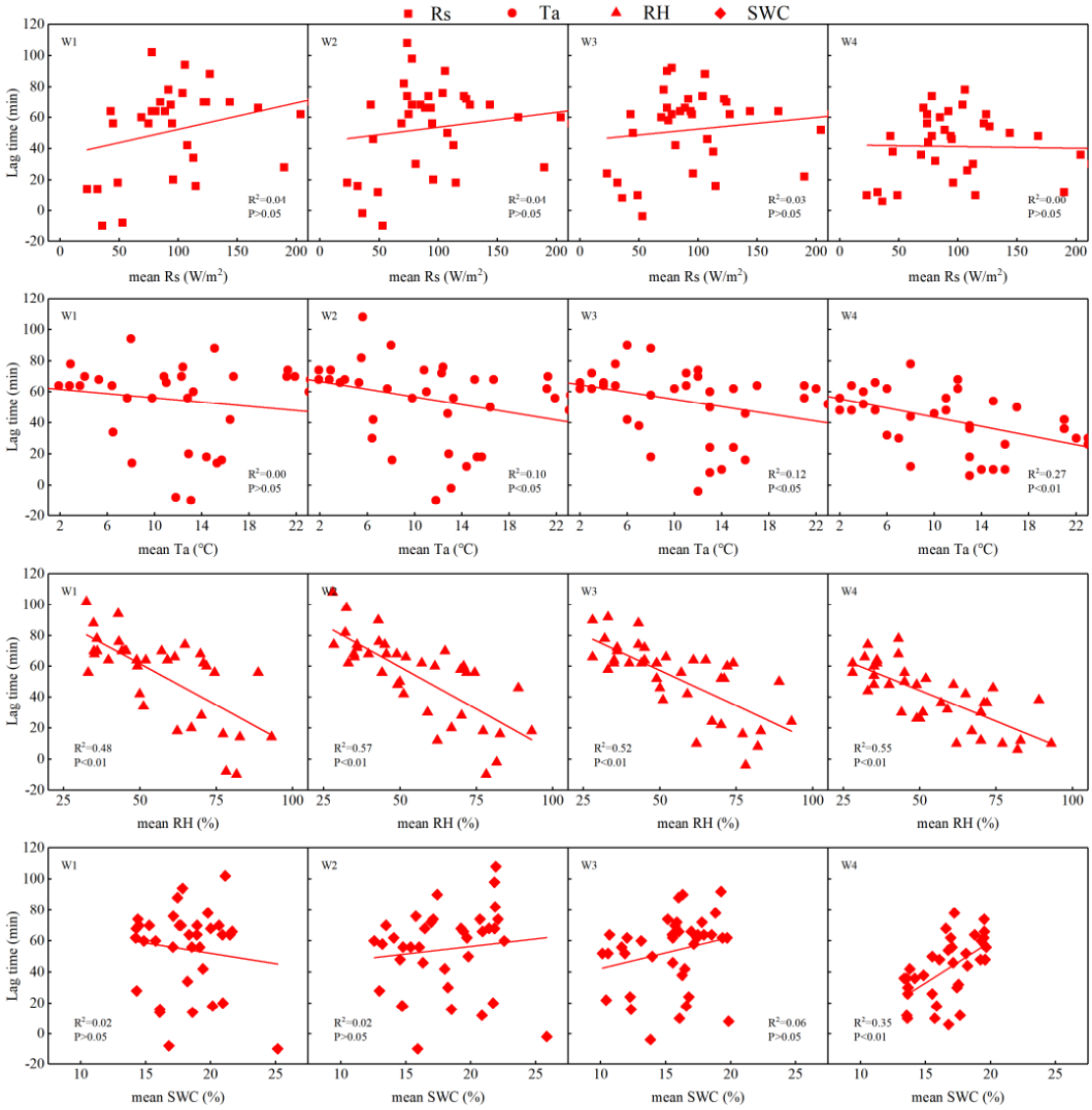

Fig.7. Relationship between LT and environmental factors on sunny days

The multiple regression analyses showed that together the daily mean Rs, Ta, RH and SWC explained 68±3, 48±8 and 64±3% of the variation of time-lag effect under rain, cloud and sun weather, respectively(Table 1). It illustrated the responding sensitivity of time-lag effect to environmental factors (Rs, Ta, RH and SWC) which varied under different weather (Fig. 8a-d). As the weather changed from rainy, cloudy to sunny, the sensitivity of TL to Rs presented first down and then maintained a steady trend, but the sensitivity of TL to RH and SWC showed a significant upward trend.

Table 4 Multiple linear regression model between LT and environmental variables, including Rs, Ta, RH and SWC.

Weather	Irrigation level	Multiple linear regression model	R^2	Significance
Rain	W1	LT=0.84+0.68Rs-0.50Ta-0.40RH-0.16SWC	0.71	$P < 0.001$
	W2	LT=0.60+0.56Rs-0.52Ta-0.08RH-0.19SWC	0.65	$P < 0.001$
	W3	LT=0.58+0.63Rs-0.77Ta+0.17RH-0.29SWC	0.71	$P < 0.001$
	W4	LT=0.42+0.59Rs-0.43Ta+0.03RH-0.04SWC	0.68	$P < 0.001$
Cloud	W1	LT=1.08+0.35Rs-0.17Ta-0.61RH-0.18SWC	0.57	$P < 0.001$

	W2	LT=0.91 +0.24Rs-0.36Ta-0.47RH-0.17SWC	0.45	$P < 0.001$
	W3	LT=0.61 +0.36Rs-0.41Ta-0.34RH+0.005SWC	0.40	$P < 0.001$
	W4	LT=0.50 +0.24Rs-0.26Ta-0.36RH+0.21SWC	0.48	$P < 0.001$
Sun	W1	LT=0.65 +0.43Rs-0.49Ta-0.40RH-0.34SWC	0.66	$P < 0.001$
	W2	LT=0.91 +0.30Rs-0.39Ta-0.49RH-0.25SWC	0.67	$P < 0.001$
	W3	LT=0.76 +0.40Rs-0.51Ta-0.43RH-0.16SWC	0.61	$P < 0.001$
	W4	LT=1.24 +0.33Rs-0.80Ta-0.56RH+0.34SWC	0.65	$P < 0.001$

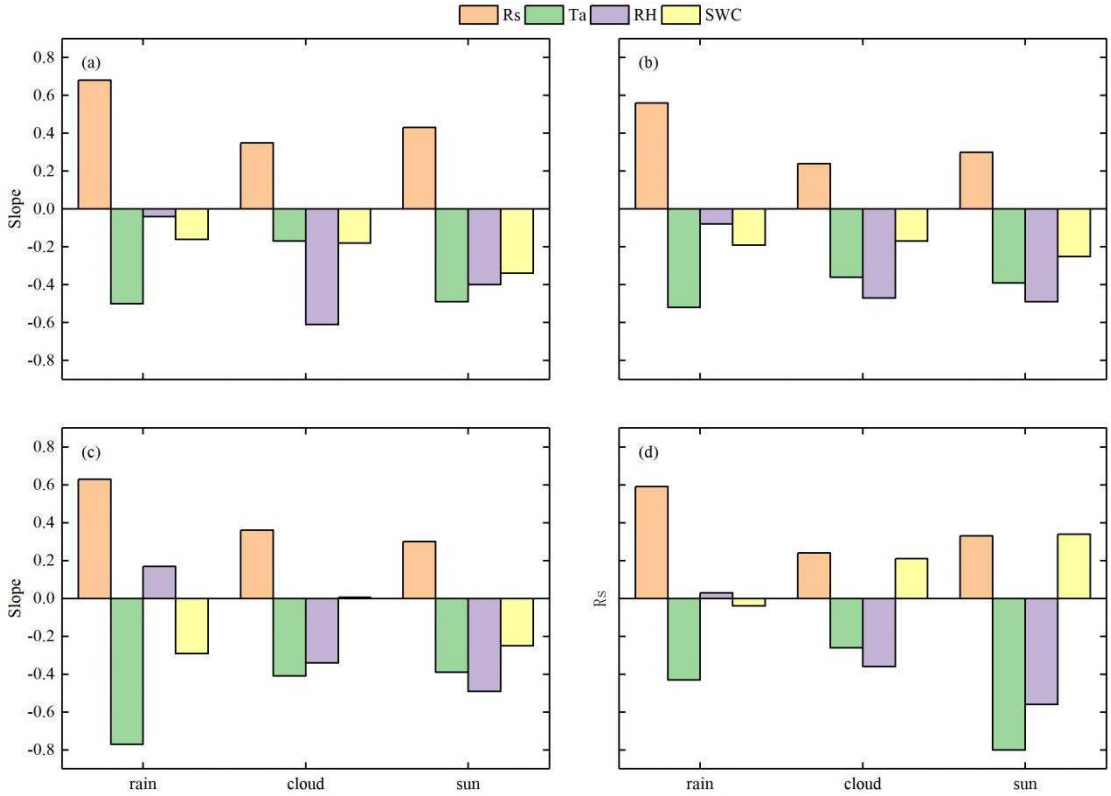

Fig.8. Sensitivity analysis of time-lag effect to environmental factors under different weather

Under rain weather, the critical factors affecting TL were Rs, Ta, RH and SWC, with the total effects of 0.73±0.03, 0.68±0.02, 0.50±0.03 and -0.50±0.08, respectively ($p < 0.01$). Rs had a significant direct effect on TL under rain weather ($p < 0.01$), while RH had a significant direct effect on TL ($p < 0.05$). Compared with results of rain weather, only SWC significantly affected TL under cloud weather, with the total effects of 0.60±0.10 ($p < 0.01$). Meanwhile, SWC had a significant direct effect on TL ($p < 0.01$), while RH had a significant direct effect on TL ($p < 0.05$). Similar to results of cloudy weather, under sun weather SWC significantly affected TL was further strengthened, with the total effects of 0.73±0.03 ($p < 0.01$). Besides, all factors had a significant direct effect on TL ($p < 0.01$).

3.4 Path analysis about TL and environmental factors

Path analysis was conducted on the four factors to study the effect of each environmental factor on the time-lag effect, and the results were shown in Table 5. Under rainy weather, Rs (ρ=0.72, p<0.01), Ta (ρ =0.68, p<0.01), RH (ρ =-0.49, p<0.01) and SWC (ρ =-0.55, p<0.01) all affected the time-lag effect. But the time-lag effect was affected in different ways. Rs and RH had a direct effect on the time-lag effect by themselves; But Ta had an indirect effect on the time-lag effect under the action of Rs; similarly, SWC has an indirect effect on the time-lag effect under the

action of Rs and RH. Under cloud weather, only RH (ρ =-0.37, p<0.05) and SWC (ρ =-0.58, p<0.01) affected the time-lag effect. Rs itself had little direct effect on the time-lag effect, and other factors had no indirect effect on Rs. Ta itself had a direct effect on the time-lag effect to a certain extent with the value of 0.31, but the indirect effect of RH on Ta was negative, eventually the direct and indirect effects offset by each other. Under sunny weather, Rs (ρ=0.89, p<0.01), Ta (ρ =-0.46, p<0.01), RH (ρ =-0.45, p<0.01) and SWC (ρ =-0.54, p<0.01) all had direct effect on the time-lag effect, but only RH and SWC had the total effect. The indirect effects of Ta and RH on Rs were negative, thus canceling out the direct effects of Rs. The same applied to Ta, the direct and indirect effects of Ta canceled each other out. The indirect effects of Rs, Ta and SWC on RH basically canceled each other, the total effect of RH on the time-lag effect did not reduce.

Table.5 Path analysis results between TL and environmental variables, including Rs, Ta, RH and SWC under different weather.

Weather	Irrigation level	Variable	Total effects	Direct effect	Indirect effect through other variables				
					Total indirect effect	Rs	Ta	RH	SWC
Rain	W1	Rs	0.74**	0.72**	0.02		-0.05	0.04	0.03
		Ta	0.68**	-0.05	0.73	0.68		0.03	0.03
		RH	-0.46**	-0.34*	-0.12	-0.09	0.00		-0.03
		SWC	-0.58**	-0.06	-0.53	-0.36	0.03	-0.19	
	W2	Rs	0.71**	0.44**	0.27		0.20	0.11	-0.05
		Ta	0.67**	0.22	0.45	0.41		0.09	-0.05
		RH	-0.53**	-0.44*	-0.10	-0.11	-0.05		0.06
		SWC	-0.51**	0.09	-0.60	-0.21	-0.11	-0.27	
	W3	Rs	0.72**	0.56**	0.15		0.16	0.11	-0.11
		Ta	0.66**	0.18	0.48	0.52		0.08	-0.12
		RH	-0.48**	-0.48*	-0.00	-0.12	-0.03		0.15
		SWC	-0.41*	0.24	-0.65	-0.26	-0.09	-0.30	
	W4	Rs	0.76**	0.63**	0.12		0.07	0.09	-0.03
		Ta	0.70**	0.07	0.62	0.59		0.07	-0.04
		RH	-0.50**	-0.37*	-0.12	-0.15	-0.01		0.04
		SWC	-0.51**	0.07	-0.58	-0.31	-0.04	-0.23	
Cloud	W1	Rs	0.14	0.22	-0.08		0.11	-0.21	0.01
		Ta	0.06	0.12	-0.06	0.20		-0.20	-0.06
		RH	-0.27*	-0.33*	0.06	0.14	0.08		-0.16
		SWC	-0.70**	-0.62**	-0.07	-0.01	0.01	-0.08	
	W2	Rs	0.12	0.070	0.05		0.30	-0.25	0.01
		Ta	0.08	0.31*	-0.23	0.06		-0.25	-0.05
		RH	-0.29*	-040*	0.11	0.05	0.19		-0.13
		SWC	-0.59**	-0.52**	-0.07	-0.00	0.03	-0.10	
	W3	Rs	0.06	0.00	0.05		0.40	-0.35	0.01
		Ta	0.05	0.43*	-0.38	0.00		-0.34	-0.04
		RH	-0.38*	-0.54**	0.17	0.00	0.27		-0.11
		SWC	-0.50**	-0.40*	-0.10	0.00	0.04	-0.15	
	W4	Rs	-0.16	-0.11	-0.05		0.34	-0.36	-0.03
		Ta	-0.16	0.37*	-0.53	-0.10		-0.35	-0.08
		RH	-0.54**	-0.56**	0.02	-0.07	0.23		-0.14
		SWC	-0.54**	-0.42*	-0.12	-0.01	0.07	-0.18	
Sun	W1	Rs	0.38*	0.97**	-0.59		-0.37	-0.29	0.07
		Ta	0.37*	-0.40*	0.78	0.90		-0.25	0.13
		RH	-0.17	-0.42**	0.25	0.68	-0.24		-0.19
		SWC	-0.69**	-0.50**	-0.20	-0.14	0.10	-0.16	
	W2	Rs	0.21	0.86**	-0.65		-0.42	-0.26	0.03
		Ta	0.22	-0.45**	0.67	0.80		-0.23	0.10
		RH	-0.32*	-0.37*	0.05	0.61	-0.28		-0.29
		SWC	-0.76**	-0.62**	-0.14	-0.05	0.08	-0.17	
	W3	Rs	0.19	0.96**	-0.77		-0.46	-0.34	0.03

		Ta	0.19	-0.50**	0.69	0.88	-0.29	0.09
		RH	-0.34*	-0.47**	0.13	0.68	-0.30	-0.25
		SWC	-0.72**	-0.54**	-0.19	-0.06	0.09	-0.22
		Rs	-0.03	0.79**	-0.82	-0.43	-0.40	0.01
	W4	Ta	-0.02	-0.47**	0.45	0.73	-0.35	0.07
		RH	-0.53**	-0.55**	0.02	0.57	-0.30	-0.25
		SWC	-0.75**	-0.53**	-0.22	-0.02	0.06	-0.26

Note: * * represents significant level P < 0.01, * represents significant level P < 0.05

4 Discussions

4.1 Time-lag effect between Tc and Ta

This study has discovered the hysteresis between Tc and Ta of winter wheat under different weather over the diel cycles (Fig. 2). Similar diel hysteresis patterns have been observed on other plants (Mahan et al., 2016; Peña Quiñones et al., 2020). For example, Hong et al. (2019) studied time-lag effect between sap flow and vapor pressure deficit of larix principis-rupprechtii mayr. However, in contrast to the previous findings, the time-lag effect in this study was investigated under different weather, and the results suggested that Ta peaked later than Tc, so the relationship between Tc and Ta showed a clockwise hysteresis cycle (Fig. 2). The lagging of Ta behind Tc was a rather common phenomenon. Tc peaked at noon (12:00~14:00) while Ta in the afternoon (13:00~16:00), hence the formation of a clockwise loop (Zhang et al., 2014). Although different weather did not change the direction of the time lag loop, a significant difference existed among sunny days, cloud days and rainy days for LT (Fig.3). Similarly, the variation of LT under different weather has also been reported by other researchers (Hong et al., 2019; Wang et al., 2019). This study showed LT on cloudy days was the longest (30~80 min), followed by sunny days (15~80 min) and rainy days (5~75 min).

On rainy days, Tc took longer to reach its peak due to insufficient Rs, so the time difference between Tc and Ta increased. However, on cloudy and sunny days, the time difference between Tc and Ta decreased when Rs met plant equilibrium demand, so Tc reached its peak earlier (Hua et al., 2009; Kuzyakov and Gavrichkova, 2010; Yu et al., 2019). In addition, compared with W4, at the irrigation levels of W1, W2 and W3, adequate soil moisture would bring the peak time of Tc forward, hence a shorter time difference between Tc and Ta. Such earlier appearance of the peak may be caused by crop evaporation capacity (Jackson, 1982). Therefore, the significant difference in time-lag effect under different weather may result from several reasons, including the meteorological factors (Hong et al., 2019), soil moisture (Zha et al., 2017) and the interaction between them (Wang et al., 2014).

4.2 Effect of meteorological factors on time-lag effect

Prior studies have pointed out the influence of meteorological factors on the lag effect (Ivanov et al., 2010; Sun et al., 2013). Hong et al. (2019) found positive correlations exist between LT and daily net solar radiation (R^2=0.33~0.37) and between LT and daily vapor pressure deficit (R^2=0.35~0.42). In contrast, Zhang et al. (2019) discovered that no significant correlation existed between lag time and meteorological factors of daily atmospheric temperature, active radiation, vapor pressure deficit and relative humidity. This contrary conclusion may arise from the failure to distinguish the effect of different weather on LT. Based on the classification of different weather, this study analyzed the correlation between meteorological factors and time-lag effect. The results showed that the time-lag effect was influenced by different meteorological factors under different weather.

On rainy days, among the factors influencing the time-lag effect, Rs was the primary factor, followed by Ta and RH (Fig.4) while on cloudy and sunny days, RH was the primary factor (Fig.5 and Fig.6). This difference may be due to the fact that the crop has not reached its upper limit of Rs absorption on rainy days and its transpiration can be further enhanced (Lundblad and Lindroth, 2002). However, on cloudy days, the crop will basically reach its upper limit of radiation absorption, so the stomata of crops may be opened, and the transpiration rate of the crop may be determined by the RH (Zhang et al., 2020). Similarly, on sunny days, RH determined the transpiration rate, and the correlation between LT and RH was further enhanced (Kimm et al., 2020).

4.3 Effect of soil moisture on time-lag effect

SWC was also identified as an important factor influencing time-lag effect between Tc and Ta, which agrees with the findings by Tuzet et al. (2003). Wullschleger et al. (1998) claimed that hysteresis was more evident in wet soil than dry soil. However, this study demonstrated no obvious difference in LT at the irrigation levels of W1, W2 and W3, but a significant downward trend of LT at W4. It indicated that the relationship between the lag time effect and the soil moisture may not be non-linear. O'Grady et al. (2008) concluded that the hysteresis did not depend on SWC when soils are wet in plantation with Eucalyptus globulus trees. Similar result was obtained in this study at W1, W2 and W3, which can meet the demand of winter wheat transportation. However, the time-lag effect was more sensitive to SWC below a certain value. This may be attributed to the fact that the water stored at W4 could not meet the demand of winter wheat transpiration during the day (Umair et al., 2019), and the stoma was only partially opened, so the peak Tc was delayed (Kaufmann, 1982).

Meanwhile, LT was poorly correlated to daily SWC at W1, W2 and W3, but highly correlated at W4, indicating that the soil moisture was a determinant for the hysteresis when soil moisture was below a threshold. Similarly, Zhang et al. (2014) pointed out that only when soil moisture is below an ecosystem-specific threshold can soil water potential be a key factor in hysteresis relation.

4.4 Effect of the coupling mechanisms between meteorological factors and soil moisture on time-lag effect

In this study, the coupling mechanisms of meteorological factors and soil moisture on the time-lag effect were different under different weather, but they displayed no significant difference at the four different irrigation levels. On rainy days, Rs and RH had direct impact on the time-lag effect while Ta and soil moisture under the action of Rs and RH had indirect impact. On cloudy days, the time-lag effect was directly influenced by RH and SWC. However, the indirect impact of RH was offset by the combined action of Rs and Ta. Furthermore, this counteracting effect was more prominent on sunny days. The indirect effects of Rs, Ta and RH were weakened mutually, so their total effects were limited. The impact of RH on soil moisture was further strengthened. This explained the variation of the sensitivity of environmental factors to time-lag effects under different weather (Fig. 8).

4.5 Caveats of the study

This study can clarify the effect of environmental factors on the time-lag effect between Tc and Ta, and further improve the monitoring accuracy of soil moisture. However, as this experiment is at the preliminary stage, application of the findings to all regions or other crops needs further study. In addition, certain correlation existed between meteorological factors and the time-lag effect, and the relationship displayed a coupling effect of multiple factors rather than linearity. Meanwhile,

the effect of SWC on time-lag effect should be divided into smaller SWC intervals so as to determine the impact of the threshold of SWC on time-lag effect. As to whether the time-lag effect can be used to monitor crop water stress effectively, future studies should involve plant physiological indicators such as leaf water potential and stomach conductance.

5. Conclusions

This study investigated the response modes of Tc and Ta with different weather and irrigation levels as well as the time-lag effect and its influencing factors. The main conclusions were as follows: 1) hysteresis existed between Tc and Ta over the diel cycles, and with different weather and irrigation levels, the time lag loop remained clockwise on winter wheat; 2) the average TL between Ta and Tc varied considerably. As the weather changed from rainy to cloudy to sunny, TL showed a downward trend. Meanwhile, no significant difference was observed on TL at the irrigation levels of W1, W2, and W3 except for W4; 3) the impacts of environmental factors on the time-lag effect were different. Rs and RH were the most important factors influencing TL on rainy days and sunny days, respectively; and Rs influenced TL indirectly via the increase of Ta and SWC on rainy days. Besides, on sunny days, RH influenced TL via the decrease of Rs and the increase of Ta and SWC. This study deepens the understanding of how environmental factors influence the time lag effect between Tc and Ta so as to further improve the monitoring accuracy of soil moisture.

Acknowledgement

This study was financially supported by the National Natural Science Foundation of China (51979232, 52179044), Natural Science Foundation in Shaanxi Province of China(2019JM-066),

References

Chen, T., De Jeu, R., Liu, Y., Van der Werf, G. and Dolman, A., 2014. Using satellite based soil moisture to quantify the water driven variability in NDVI: A case study over mainland Australia. Remote Sensing of Environment, 140: 330-338.

Clawson, K., Jackson, R. and Pinter, P., 1989. Evaluating plant water stress with canopy temperature differences.

Hong, L. et al., 2019. Time-Lag effect between sap flow and environmental factors of Larix principis-rupprechtii Mayr. Forests, 10(11): 971.

Jackson, R.D., 1982. Canopy temperature and crop water stress, Advances in irrigation. Elsevier, pp. 43-85.

Jackson, R.D., Idso, S., Reginato, R. and Pinter Jr, P., 1981. Canopy temperature as a crop water stress indicator. Water resources research, 17(4): 1133-1138.

Zhou, Y. et al., 2021. Diagnosis of winter-wheat water stress based on UAV-borne multispectral image texture and vegetation indices. Agricultural Water Management, 256: 107076.

Alados, I., Foyo-Moreno, I., Olmo, F. and Alados-Arboledas, L., 2003. Relationship between net radiation and solar radiation for semi-arid shrub-land. Agricultural and Forest Meteorology, 116(3-4): 221-227.

Anderson, L.O. et al., 2010. Remote sensing detection of droughts in Amazonian forest canopies. New Phytologist, 187(3): 733-750.

Baker, J.M., Noman, J.M. and Kano, A., 2001. A new approach to infrared thermometry. Agricultural and forest meteorology, 108(4): 281-292.

421 Biju, S., Fuentes, S. and Gupta, D., 2018. The use of infrared thermal imaging as a non-destructive
422 screening tool for identifying drought-tolerant lentil genotypes. Plant physiology and
423 biochemistry, 127: 11-24.
424 Bo, X., Du, T., Ding, R. and Comas, L., 2017. Time lag characteristics of sap flow in seed-maize and
425 their implications for modeling transpiration in an arid region of Northwest China. Journal of
426 Arid Land, 9(4): 515-529.
427 Chen, T., De Jeu, R., Liu, Y., Van der Werf, G. and Dolman, A., 2014. Using satellite based soil
428 moisture to quantify the water driven variability in NDVI: A case study over mainland
429 Australia. Remote Sensing of Environment, 140: 330-338.
430 Clawson, K., Jackson, R. and Pinter, P., 1989. Evaluating plant water stress with canopy temperature
431 differences.
432 Davis, M.B., 1989. Lags in vegetation response to greenhouse warming. Climatic change, 15(1): 75-82.
433 Gerhards, M. et al., 2018. Analysis of airborne optical and thermal imagery for detection of water stress
434 symptoms. Remote Sensing, 10(7): 1139.
435 Hayat, M. et al., 2020. A multiple-temporal scale analysis of biophysical control of sap flow in Salix
436 psammophila growing in a semiarid shrubland ecosystem of northwest China. Agricultural
437 and Forest Meteorology, 288: 107985.
438 Hong, L. et al., 2019. Time-Lag effect between sap flow and environmental factors of Larix
439 principis-rupprechtii Mayr. Forests, 10(11): 971.
440 Hua, W. et al., 2009. Time lag characteristics of stem sap flow of common tree species during their
441 growth season in Beijing downtown. Yingyong Shengtai Xuebao, 20(9).
442 Ivanov, V.Y. et al., 2010. Hysteresis of soil moisture spatial heterogeneity and the “homogenizing”
443 effect of vegetation. Water Resources Research, 46(9).
444 Jackson, R.D., Idso, S., Reginato, R. and Pinter Jr, P., 1981. Canopy temperature as a crop water stress
445 indicator. Water resources research, 17(4): 1133-1138.
446 Jiang, S. et al., 2022. Leaf-and ecosystem-scale water use efficiency and their controlling factors of a
447 kiwifruit orchard in the humid region of Southwest China. Agricultural Water Management,
448 260: 107329.
449 Kaufmann, M.R., 1982. Evaluation of season, temperature, and water stress effects on stomata using a
450 leaf conductance model. Plant Physiology, 69(5): 1023-1026.
451 Khazaie, H., Mohammady, S., Monneveux, P. and Stoddard, F., 2011. The determination of direct and
452 indirect effects of carbon isotope discrimination (Δ), stomatal characteristics and water use
453 efficiency on grain yield in wheat using sequential path analysis. Australian Journal of Crop
454 Science, 5(4): 466-472.
455 Kimm, H. et al., 2020. Redefining droughts for the US Corn Belt: The dominant role of atmospheric
456 vapor pressure deficit over soil moisture in regulating stomatal behavior of Maize and
457 Soybean. Agricultural and Forest Meteorology, 287: 107930.
458 Kuzyakov, Y. and Gavrichkova, O., 2010. Time lag between photosynthesis and carbon dioxide efflux
459 from soil: a review of mechanisms and controls. Global Change Biology, 16(12): 3386-3406.
460 Lu, C.-G., Xia, S.-j., Jing, C., Ning, H. and Yao, K.-m., 2008. Plant temperature and its simulation
461 model of thermo-sensitive genic male sterile rice. Rice Science, 15(3): 223-231.
462 Lundblad, M. and Lindroth, A., 2002. Stand transpiration and sapflow density in relation to weather,
463 soil moisture and stand characteristics. Basic and Applied Ecology, 3(3): 229-243.

464 Mahan, J.R., Payton, P.R. and Laza, H.E., 2016. Seasonal canopy temperatures for normal and okra leaf
465 cotton under variable irrigation in the field. Agriculture, 6(4): 58.
466 Meinzer, F.C., James, S.A. and Goldstein, G., 2004. Dynamics of transpiration, sap flow and use of
467 stored water in tropical forest canopy trees. Tree physiology, 24(8): 901-909.
468 O'Grady, A.P., Worledge, D. and Battaglia, M., 2008. Constraints on transpiration of Eucalyptus
469 globulus in southern Tasmania, Australia. Agricultural and Forest Meteorology, 148(3):
470 453-465.
471 Oogathoo, S., Houle, D., Duchesne, L. and Kneeshaw, D., 2020. Vapour pressure deficit and solar
472 radiation are the major drivers of transpiration of balsam fir and black spruce tree species in
473 humid boreal regions, even during a short-term drought. Agricultural and Forest Meteorology,
474 291: 108063.
475 Peña Quiñones, A.J., Hoogenboom, G., Salazar Gutiérrez, M.R., Stöckle, C. and Keller, M., 2020.
476 Comparison of air temperature measured in a vineyard canopy and at a standard weather
477 station. Plos one, 15(6): e0234436.
478 Ru, C. et al., 2020. Evaluation of the Crop Water Stress Index as an Indicator for the Diagnosis of
479 Grapevine Water Deficiency in Greenhouses. Horticulturae, 6(4): 86.
480 Saatchi, S. et al., 2013. Persistent effects of a severe drought on Amazonian forest canopy. Proceedings
481 of the National Academy of Sciences, 110(2): 565-570.
482 Seber, G.A. and Lee, A.J., 2012. Linear regression analysis, 329. John Wiley & Sons.
483 Sun, J.-y., Sun, X.-y., Hu, Z.-y. and Wang, G.-x., 2020. Exploring the influence of environmental
484 factors in partitioning evapotranspiration along an elevation gradient on Mount Gongga,
485 eastern edge of the Qinghai-Tibet Platea, China. Journal of Mountain Science, 17(2): 384-396.
486 Sun, J., Liu, Z., Xiao, J., Duan, A. and Zhang, S., 1998. Study on upper and lower limits of suitable soil
487 moisture for water-saving irrigation of winter wheat China Rural Water and Hydropower, 9:
488 10-12.
489 Sun, T., Wang, Z.H. and Ni, G.H., 2013. Revisiting the hysteresis effect in surface energy budgets.
490 Geophysical Research Letters, 40(9): 1741-1747.
491 Tamai, K., Abe, T., Araki, M. and Ito, H., 1998. Radiation budget, soil heat flux and latent heat flux at
492 the forest floor in warm, temperate mixed forest. Hydrological processes, 12(13‐14):
493 2105-2114.
494 Tranmer, M. and Elliot, M., 2008. Multiple linear regression. The Cathie Marsh Centre for Census and
495 Survey Research (CCSR), 5(5): 1-5.
496 Tuzet, A., Perrier, A. and Leuning, R., 2003. A coupled model of stomatal conductance, photosynthesis
497 and transpiration. Plant, Cell & Environment, 26(7): 1097-1116.
498 Umair, M. et al., 2019. Water-saving potential of subsurface drip irrigation for winter wheat.
499 Sustainability, 11(10): 2978.
500 Vicente-Serrano, S.M. et al., 2013. Response of vegetation to drought time-scales across global land
501 biomes. Proceedings of the National Academy of Sciences, 110(1): 52-57.
502 Wang, B. et al., 2014. Soil moisture modifies the response of soil respiration to temperature in a desert
503 shrub ecosystem. Biogeosciences, 11(2): 259-268.
504 Wang, H., Tetzlaff, D. and Soulsby, C., 2019. Hysteretic response of sap flow in Scots pine (Pinus
505 sylvestris) to meteorological forcing in a humid low‐energy headwater catchment.
506 Ecohydrology, 12(6): e2125.

Wu, D. et al., 2015. Time‐lag effects of global vegetation responses to climate change. Global change biology, 21(9): 3520-3531.

Wullschleger, S.D., Hanson, P.J. and Tschaplinski, T.J., 1998. Whole-plant water flux in understory red maple exposed to altered precipitation regimes. Tree Physiology, 18(2): 71-79.

Xing, X., Liu, Y., Yu, M. and Ma, X., 2016. Determination of dominant weather parameters on reference evapotranspiration by path analysis theory. Computers and Electronics in Agriculture, 120: 10-16.

Yu, M.-H., Ding, G.-D., Gao, G.-L., Zhao, Y.-Y. and Sai, K., 2019. Hysteresis resulting in forestry heat storage underestimation: A case study of plantation forestry in northern China. Science of The Total Environment, 671: 608-616.

Zha, T. et al., 2017. Soil moisture control of sap-flow response to biophysical factors in a desert-shrub species, Artemisia ordosica. Biogeosciences, 14(19).

Zhai, J.-l., Feng, R.-g. and Xia, J., 2003. Constraining factors to sustainable utilization of water resources and their countermeasures in China. Chinese Geographical Science, 13(4): 310-316.

Zhang, B. et al., 2016. Multi-scale evapotranspiration of summer maize and the controlling meteorological factors in north China. Agricultural and Forest Meteorology, 216: 1-12.

Zhang, J., Wang, L. and Su, J., 2018a. The soil water condition of a typical agroforestry system under the policy of Northwest China. Forests, 9(12): 730.

Zhang, Q., Manzoni, S., Katul, G., Porporato, A. and Yang, D., 2014. The hysteretic evapotranspiration—Vapor pressure deficit relation. Journal of Geophysical Research: Biogeosciences, 119(2): 125-140.

Zhang, Q. et al., 2018b. Changes in photosynthesis and soil moisture drive the seasonal soil respiration-temperature hysteresis relationship. Agricultural and Forest Meteorology, 259: 184-195.

Zhang, R. et al., 2019. Hysteresis in sap flow and its controlling mechanisms for a deciduous broad-leaved tree species in a humid karst region. Science China Earth Sciences, 62(11): 1744-1755.

Zhang, X. et al., 2020. Stomatal conductance bears no correlation with transpiration rate in wheat during their diurnal variation under high air humidity. PeerJ, 8: e8927.

Zhao, P., Rao, X.-Q., Ma, L., Cai, X.-A. and Zeng, X.-P., 2006. The variations of sap flux density and whole-tree transpiration across individuals of Acacia mangium. Acta Ecologica Sinica, 12: 4050-4058.

Zhou, S., Hu, X., Zhou, Z., Wang, W.e. and Ran, H., 2019. Improving water use efficiency of spring maize by adopting limited supplemental irrigation following sufficient pre-sowing irrigation in Northwest China. Water, 11(4): 802.

Zhou, Y. et al., 2021. Diagnosis of winter-wheat water stress based on UAV-borne multispectral image texture and vegetation indices. Agricultural Water Management, 256: 107076.